Molecular Biology of the Cell
Vol. 17, 749–759, February 2006

RhoA GTPase Regulates M-Cadherin Activity and Myoblast Fusion[D] [V]

Sophie Charrasse,* Franck Comunale,* Yaël Grumbach,* Francis Poulat,† Anne Blangy,* and Cécile Gauthier-Rouvière*

*Centre de Recherches de Biochimie Macromoléculaire, Centre National de la Recherche Scientifique Formation de Recherche en Evolution 2593, 34293 Montpellier Cedex, France; and †Institut de Génétique Humaine, Centre National de la Recherche Scientifique Unité Propre de Recherche 1142, 34396 Montpellier Cedex 5, France

Submitted April 6, 2005; Revised October 11, 2005; Accepted November 3, 2005
Monitoring Editor: Ben Margolis

The Rho family of GTP-binding proteins plays critical roles during myogenesis induction. To elucidate their role later during myogenesis, we have analyzed RhoA function during myoblast fusion into myotubes. We find that RhoA activity is rapidly and transiently increased when cells are shifted into differentiation medium and then is decreased until myoblast fusion. RhoA activity must be down-regulated to allow fusion, because expression of a constitutively active form of RhoA (RhoAV14) inhibits this process. RhoAV14 perturbs the expression and localization of M-cadherin, a member of the Ca^{2+}-dependent cell–cell adhesion molecule family that has an essential role in skeletal muscle cell differentiation. This mutant does not affect N-cadherin and other proteins involved in myoblast fusion, β1-integrin and ADAM12. Active RhoA induces the entry of M-cadherin into a degradative pathway and thus decreases its stability in correlation with the monoubiquitination of M-cadherin. Moreover, p120 catenin association with M-cadherin is decreased in RhoAV14-expressing cells, which is partially reverted by the inhibition of the RhoA effector Rho-associated kinase ROCK. ROCK inhibition also restores M-cadherin accumulation at the cell–cell contact sites. We propose that the sustained activation of the RhoA pathway inhibits myoblast fusion through the regulation of p120 activity, which controls cadherin internalization and degradation.

INTRODUCTION

The development of skeletal muscle is a multistep process in which pluripotent mesodermal cells give rise to myoblasts. After this specification step, myoblasts delaminate, migrate, and proliferate until they reach their sites of differentiation, where they differentiate and fuse into myotubes that mature to finally form multinucleated muscle fibers (Andres and Walsh, 1996; Taylor, 2000). Each step of this process is highly regulated and although the molecular mechanisms that regulate myogenesis induction are starting to be elucidated, little is known about myoblast fusion. Myoblast fusion is a stepwise process involving the initial recognition and adhesion between fusion-competent myoblasts, subsequent myoblast alignment, and finally membrane breakdown and fusion (Doberstein *et al*., 1997). This process also occurs when satellite cells fuse with damaged membranes to regenerate muscle fibers. Myoblast fusion has been studied in mammalian myoblastic cell lines, mice, and *Drosophila*, and some of the molecules involved have been identified. Genetic screens and biochemical analyses have identified many proteins involved in muscle cell fusion located at the cell surface, in the cytoplasm, and in the nucleus (reviewed in Dworak and Sink, 2002; Taylor, 2002). The membrane proteins implicated in myotube formation in vertebrates include β1 integrin, ADAM12 (a member of a disintegrin and metalloproteinase family), NCAM, and M-cadherin (Rosen *et al*., 1992; Zeschnigk *et al*., 1995; Fazeli *et al*., 1996; Huovila *et al*., 1996; Charlton *et al*., 2000; Schwander *et al*., 2003). M-cadherin belongs to the cadherin family of calcium-dependent adhesion molecules. The N-terminal extracellular domain mediates homophilic binding, and the intracellular region binds to β- and γ- and p120 catenins. α-Catenin interacts with β- and γ-catenins and the actin microfilaments. M-cadherin is found predominantly in developing skeletal muscles and is highly expressed during secondary myogenesis. In mature skeletal muscle, M-cadherin is detectable in satellite cells and on the sarcolemma of myofibers underlying satellite cells (Moore and Walsh, 1993; Bornemann and Schmalbruch, 1994; Rose *et al*., 1994; Cifuentes-Diaz *et al*., 1995). M-cadherin is also found at neuromuscular junctions, intramuscular nerves, and in two regions of the central nervous system, namely, the spinal cord and the cerebellum (Cifuentes-Diaz *et al*., 1996; Bahjaoui-Bouhaddi *et al*., 1997). M-cadherin-deficient mice show no defect in skeletal muscle development, probably because of compensation by other cadherin molecules, in particular N-cadherin (Hollnagel *et al*., 2002). However, various studies in cultured myoblasts have postulated that M-cadherin may be essential for the fusion of myoblast to myotubes (Donalies *et al*., 1991; Pouliot *et al*., 1994; Zeschnigk *et al*., 1995; Kuch *et al*., 1997). In addition to cell surface molecules, certain signaling pathways have been implicated in myoblast fusion (Chen and Olson, 2004). In

This article was published online ahead of print in *MBC in Press* (http://www.molbiolcell.org/cgi/doi/10.1091/mbc.E05–04–0284) on November 16, 2005.

[D] [V] The online version of this article contains supplemental material at *MBC Online* (http://www.molbiolcell.org).

Address correspondence to: Cécile Gauthier-Rouvière (cecile.gauthier@crbm.cnrs.fr).

particular, we have shown that RhoA, a member of the Rho GTPase family that is a positive regulator of myogenesis induction, prevents myoblast fusion (Meriane *et al*., 2000), which was recently confirmed by others (Nishiyama *et al*., 2004). Cross-talk between Rho GTPases and cadherin molecules has been described in many cases (Charrasse *et al*., 2002). In the present study, we have investigated the effect of RhoA activation on M-cadherin activity in mouse C2C12 myoblasts. We find that RhoA activity is decreased at the onset of myoblast fusion and that the expression of a constitutive active form of RhoA (RhoAV14) totally inhibits the fusion process. RhoAV14 expression specifically decreases the level of M-cadherin without affecting another molecule of the family, N-cadherin, or β1-integrin and ADAM12, two proteins involved in myoblast fusion. M-cadherin localization is also perturbed in RhoAV14-expressing cells. RhoA induces the ubiquitination and degradation of M-cadherin through a lysosomal-dependent pathway. Finally, we observe that RhoAV14, through the activation of its effector, the Rho-associated kinase ROCK, decreases p120 catenin association with M-cadherin.

MATERIALS AND METHODS

DNA Constructs

Construct encoding RhoA has been described previously (Gauthier-Rouviere *et al*., 1998). The complete murine M-cadherin coding sequence (accession no. NM_007662) was cloned into the pEGFP-N1 vector (Clontech, Mountain View, CA) using the *Nhe*I and *Sac*II sites. The characterization of this construct is shown in Supplemental Data #1. Green fluorescent protein-tagged cystinosin (CTNS-GFP) was kindly provided by Viki Kalatzis (Centre National de la Recherche Scientifique, Montpellier, France).

Establishment of Stable Cell Lines

G418-resistant GP+E-86 clones expressing constitutively activate form of RhoA (RhoAV14) were grown to collect retrovirus-containing cell-free supernatants. Infection of C2C12 myoblasts was performed as described previously (Meriane *et al*., 2000). Cells were grown continuously in G418.

Cell Culture

C2C12 mouse myoblasts were grown in DMEM/Ham's F-12 (1:1) supplemented with 10% fetal calf serum (FCS) (Hyclone/Perbio Sciences, Brebieres, France). To induce differentiation growth, medium was replaced with differentiation medium consisting of DMEM/Ham's F-12 supplemented with 2% FCS. Stable cell lines derived from C2C12 myoblasts were cultured under the same conditions in medium supplemented with 1 mg/ml G418. HeLa cells (American Type Culture Collection, Manassas, VA) were grown in DMEM supplemented with 10% FCS. The ROCK inhibitor Y-27632 (Sigma-Aldrich, St. Louis, MO) was used at 5 μm for 2–3 h. Chloroquine (Sigma-Aldrich) was used at 100 μM. LysoTracker DND99 (Invitrogen, Cergy Pontoise, France) was used at 50 nM. Fresh cycloheximide (CHX) diluted in phosphate-buffered saline (PBS) was used at 10 μg/ml.

Polyclonal Anti-M-Cadherin Antibody Production

The 750-1765 fragment of M-cadherin (NM_007662) corresponding to amino acids 250–590 was cloned in the pGEX5X-2 vector. GST-M-cadherin fragment was produced as described previously (Mary *et al*., 2002). Three rabbits were injected with 80–100 μg of glutathione *S*-transferase (GST)-M-cadherin protein. Antisera were tested by immunoblotting and immunocytochemistry. Affinity purification was performed by incubation with the GST-M-cadherin fragment spotted onto nitrocellulose. The characterization of this antibody is shown in Supplemental data #2.

Gel Electrophoresis and Immunoblotting

Cell extracts were prepared as described previously (Charrasse *et al*., 2002). Protein concentration was determined with a BCA protein assay kit (Pierce Chemical, Rockford, IL). Protein (20 μg) was resolved on polyacrylamide gel (8 and 12%) and transferred onto Immobilon-P. Membranes were incubated with monoclonal antibodies against N-cadherin (1:2000), β1-integrin (1:2500) (both from BD Transduction Laboratories, Lexington, KY), troponin T (1:1000), myosin (1:2000) (both from Sigma-Aldrich), myogenin (1:500) (BD Biosciences PharMingen, San Diego, CA), and α-tubulin (1:100) or with polyclonal (1:1000) or monoclonal (1:200; NanoTools, Munich, Germany) anti-M-cadherin antibody. Membranes were processed as described previously (Charrasse *et al*., 2002).

Pulse-Chase Experiments

Control and RhoAV14-expressing C2C12 myoblasts where incubated for 30 min in methionine-free media (DMEM minus methionine, 2 mM glutamine, and 2% dialyzed FCS) and pulse labeled for 30 min with 1 mCi/ml [^{35}S]methionine/cysteine (Promix 35S; GE Healthcare, Little Chalfont, Buckinghamshire, United Kingdom). Cells where washed twice in ice-cold PBS and resuspended in complete DMEM/Ham's F-12 medium. At indicated time, cells where harvested and lysed in immunoprecipitation buffer. Extracts were immunoprecipitated using an anti-M-cadherin polyclonal antibody (1/50), separated on an 8% acrylamide gel that was treated with Amplify (GE Healthcare). Radioactive bands were visualized by autoradiography with phosphorscreens and a PhosphorImager (GE Healthcare) and quantified using ImageQuant (GE Healthcare).

Immunoprecipitation

C2C12 cells were cotransfected with ubiquitin-hemagglutinin (HA)-tagged vector (kindly provided by Isabelle Jariel-Encontre, Centre National de la Recherche Scientifique) and with cytomegalovirus-β-galactosidase vector (1/5) to normalize transfection efficiency. Then, cells were lysed for 10 min in ice-cold extraction protein buffer (Charrasse *et al*., 2002). Extracts normalized with the amount of β-galactosidase were immunoprecipitated using a mouse monoclonal anti-HA antibody from ascites (1/500 dilution), separated on a polyacrylamide gel, and then transferred onto nitrocellulose. Membranes were probed with M-cadherin antibody followed by peroxidase-conjugated anti-rabbit antibody (GE Healthcare). To analyze M-cadherin/p120 catenin and N-cadherin/p120 complexes, monoclonal p120 antibody (BD Transduction Laboratories) was used for immunoprecipitation, and either M-cadherin or N-cadherin detection was performed using monoclonal antibody (1/1000) (BD Transduction Laboratories).

Cell Surface Biotinylation

C2C12 cells grown on 60-mm dishes were incubated with 1 mg/ml sulfosuccinimidyl 2-(biotinamido) ethyl-dithioproprionate (sulfo-NHS-SS-biotin) (Pierce Chemical), followed by washing with sulfo-NHS-SS-biotin blocking reagent (50 mM NH_4Cl in PBS containing 1 mM $MgCl_2$ and 0.1 mM $CaCl_2$) to quench free sulfo-NHS-SS-biotin, followed by several further washes in PBS (Le *et al*., 1999). Cells were then scrapped and lysed as described above before centrifugation to obtain a detergent-soluble supernatant. At this stage, an aliquot of 10 μl was kept (=total fraction), and the remainder was incubated with streptavidin beads to collect biotinylated proteins. Samples were then analyzed by SDS-PAGE and immunoblotting to identify M-cadherin. Different luminescence exposures were collected, and exposures in the linear range were used. Quantification was performed using Aida/2D densitometry software from at least five independent experiments.

siRNA Transfection

Short interfering RNA (siRNA) constructs were made in pSUPER polymerase III expression vector (Charrasse *et al*., 2004). To suppress endogenous M-cadherin expression, oligonucleotide GATCCCC**CAGCAGCTAGGCAGTGTCA**ttcaagaga**TGACACTGCCTA GCTGCTG**TTTTTGGAAA was inserted into pSUPER. Bold letters correspond to oligonucleotides 735–753 of the mouse M-cadherin cDNA sequence (NM_007662). As a control, R-cadherin siRNA was used (Charrasse *et al*., 2004). Cells (25,000) were plated in six-well Limbro 1 d before transfection. A first transfection was performed in 20–30% confluent cells with a construct encoding empty pEGFP and either the M-cadherin siRNA or the R-cadherin siRNA (1:5). A second transfection was performed 24 h later when cells were 50–60% confluent. Twenty-four hours after the second transfection, cells from two wells were mixed before addition of differentiation medium. For all transfections, LipofectAMINE (Invitrogen) was used.

Immunocytochemistry

Cells growing onto 35-mm dishes were fixed in 3.7% formaldehyde in PBS followed by a 5-min permeabilization in 0.1% Triton X-100 in PBS and incubated in PBS containing 0.1% bovine serum albumin. Transferrin receptor antibody was from Zymed Laboratories (South San Francisco, CA). Anti-M-cadherin was revealed by either an Alexa Fluor 546-or an Alexa Fluor 488-conjugated goat anti-rabbit antibody (Molecular Probes, Interchim, Montluçon, France). Cells were analyzed as previously described (Charrasse *et al*., 2002, 2003, 2004).

To label lysosomes, cells were transfected with CTNS-GFP (Kalatzis *et al*., 2001) or incubated with LysoTracker DND99 (Invitrogen).

Single plane images were captured using a MicroMax 1300 charge-coupled device camera (Princeton Instruments, Trenton, NJ) driven by MetaMorph (Molecular Devices, Sunnyvale, CA) software. Images were deconvolved using the maximum likelihood estimation algorithm (Huygens; Scientific Volume Imaging, Hilversum, The Netherlands). The restored images were saved as Tif files that were mounted using Adobe Photoshop and Adobe Illustrator (Adobe Systems, Mountain View, CA).

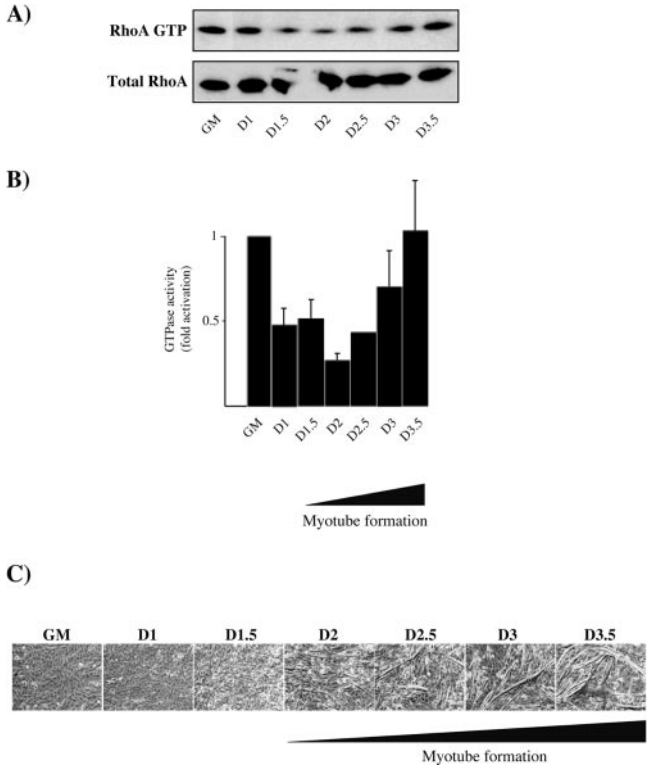

Figure 1. Variation of RhoA activity during myogenesis. (A) The level of GTP-bound RhoA was measured using GST fused to the Rho-binding domain of the RhoA effector Rhotekin (GST-TRBD) in lysates obtained from cells in growth medium or differentiation medium collected at the indicated times (1–3.5 d after addition of the differentiation medium). RhoA was detected by immunoblotting. (B) Three independent experiments were analyzed by densitometry, as described in *Materials and Methods*. The histogram represents the GTPase activity normalized to the amount of total protein. GM, growth medium D, day. (C) Phase contrast images of myoblasts and myotubes during the differentiation process. For each panel, cells are representative of three independent experiments. Bar, 10 μm.

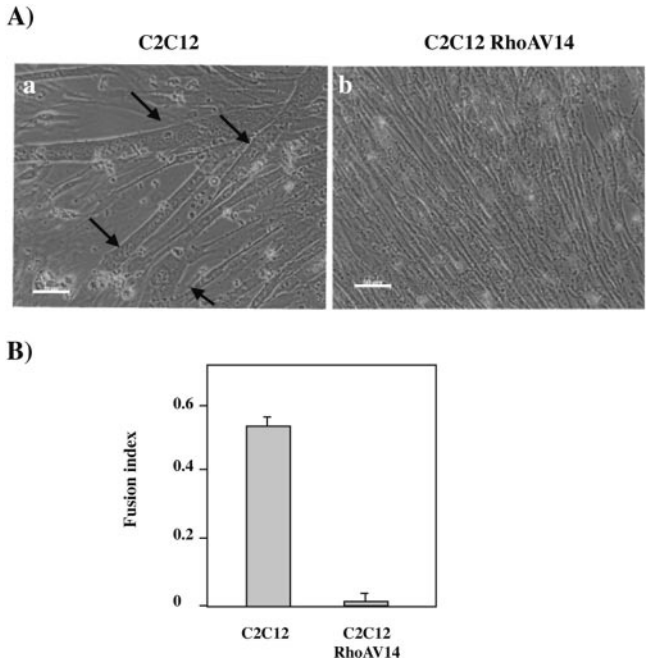

Figure 2. Effect of RhoAV14 on myoblast fusion. (A) C2C12 myoblasts expressing RhoAV14 were grown to 80% confluence and shifted to differentiation medium for 4 d. Phase contrast images show the presence of myotubes in control C2C12 myoblasts (arrows in a), whereas C2C12 RhoAV14 myoblasts align but not fuse (b). Bar, 50 μm. (B) The fusion index, i.e., the number of nuclei in multinucleated myotubes divided by the total number of nuclei, was calculated for control and RhoAV14-expressing myoblasts. The histogram represents the fusion index calculated from three independent experiments, where ~1000 nuclei were counted.

Time-Lapse Imaging

Time-lapse epifluorescence microscopy was performed as described previously (Mary *et al*., 2002). For confocal acquisition, a spinning Nipkow disk was used. Time series of captured images were deconvolved, and restored images were saved as Tif files that were compiled into QuickTime movies using MetaMorph.

RhoA GTPase Activity Assay

C2C12 myoblasts either in proliferation or during the course of differentiation were lysed and processed to measure the total and GTP RhoA level as described previously (Charrasse *et al*., 2002).

RESULTS

RhoA GTPase Activity Decreases at the Onset of Myoblast Fusion

RhoA is an integral part of the skeletal muscle differentiation pathway and plays an obligatory role during myogenic induction (Carnac *et al*., 1998; Wei *et al*., 1998; Meriane *et al*., 2000). In addition, the level of RhoA GTP is increased by a pathway that promotes the commitment to myogenesis (Charrasse *et al*., 2003). We measured RhoA activation at different times after the shift to differentiation medium using pull-down assays (Figure 1, A and B). RhoA GTP levels are substantially reduced after 2 d in differentiation medium (DM), which corresponds to the onset of the fusion process as shown by the morphological analysis of myoblast differentiation (Figure 1C).

Expression of Constitutively Active RhoA Inhibits Myoblast Fusion

We next investigated the effects of the expression of constitutively active RhoA (V14) on myoblast fusion. For this purpose, we have generated stable C2C12 myoblast cell lines using retroviruses encoding myc-tagged RhoAV14. As previously shown using L6 myoblasts (Meriane *et al*., 2000), we observed that RhoAV14 potentiates the differentiation process because myogenin, troponin T, and myosin heavy chain expression was accelerated (our unpublished data). Interestingly, we were unable to detect any myotube formation, as shown microscopically 4 d after DM addition where cells stay aligned and elongated (Figure 2A) and by the measurement of the fusion index (Figure 2B). No myotubes were observed even after 7 d in DM, indicating that the myoblast to myotube transition is effectively blocked and not simply delayed (our unpublished data).

M-Cadherin Is Required for Myoblast Fusion

A previous report has proposed a role for M-cadherin during the fusion process (Zeschnigk *et al*., 1995). Curiously, mice lacking M-cadherin do not present defects in muscle development, and the authors proposed that this might reflect compensation by N-cadherin (Hollnagel *et al*., 2002). Because the first study was performed in L6 myoblasts

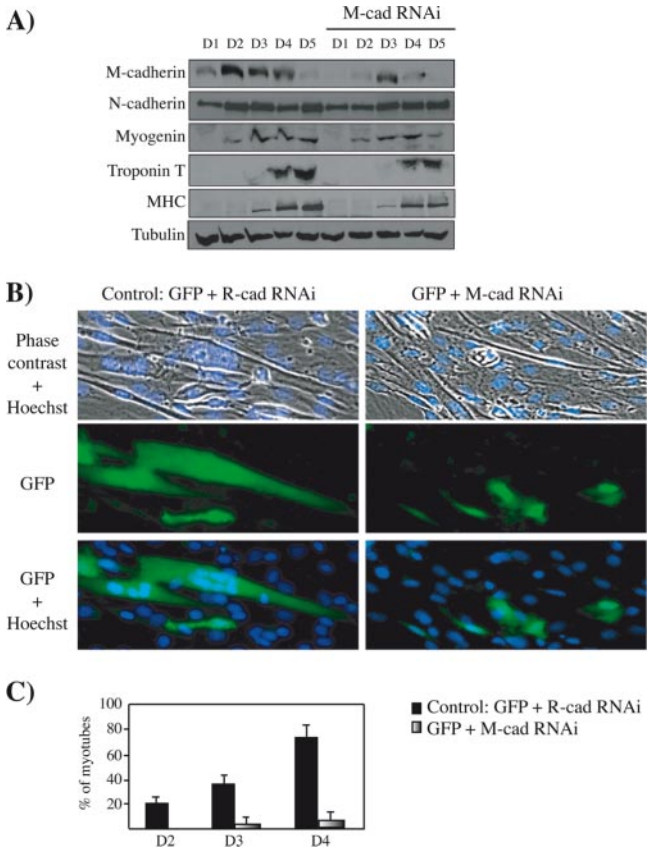

Figure 3. Inhibition of M-cadherin expression by RNAi prevents myotube formation. (A) M-cadherin siRNA interferes with M-cadherin protein expression without affecting N-cadherin, myogenin, troponin T, MHC, and α-tubulin expression. Expression of these proteins was analyzed by Western blot during differentiation of C2C12 cells and C2C12 transfected twice with pSuper driving the expression of M-cadherin siRNA. (B) Inhibition of M-cadherin by RNAi prevents myotube formation. C2C12 cells coexpressing empty pEGFP with either R-cadherin siRNA (a–c) or M-cadherin siRNA (d–f) were fixed after 4 d in DM. Shown are overlays of phase contrast image and DNA staining (a and d), GFP expression (b and e), and overlays of GFP expression and DNA staining (c and f). Bar, 20 μm. (C) Values represent the percentage of myotubes in GFP- and RNAi-coexpressing cells during the differentiation process. The results are representative of three independent experiments, each involving ~100 transfected cells.

lacking N-cadherin, it was important to know whether M-cadherin is required for myoblast fusion in C2C12 myoblasts, which express both N- and M-cadherins. For this purpose, we used RNA interference technology to lower M-cadherin expression. M-cadherin silencing was analyzed by Western blot during the differentiation process of C2C12 myoblasts (Figure 3A). M-cadherin protein levels were strongly decreased during myogenesis by RNA interference (RNAi). In contrast, N-cadherin and tubulin expression were unaffected, demonstrating the specificity of the RNAi. Interestingly, the expression of the myogenic marker myogenin, troponin T, and myosin heavy chain (MHC) was not affected by M-cadherin gene silencing, indicating that induction of these genes does not require M-cadherin. In contrast, M-cadherin knockdown specifically inhibits myotube formation (Figure 3, B and C). Cells cotransfected with empty GFP and control R-cadherin RNAi were able to fuse, whereas cells cotransfected with empty GPF and M-cadherin RNAi

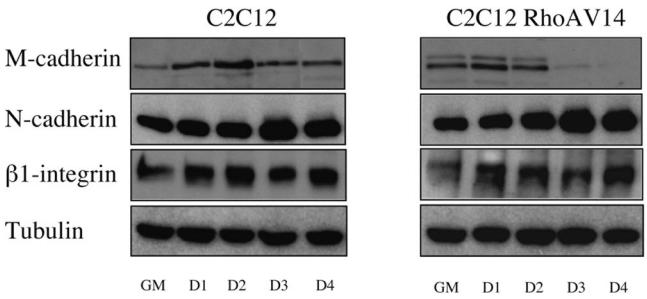

Figure 4. Effect of RhoAV14 on M-cadherin expression. Protein extracts (20 μg/well) from parental C2C12 and C2C12 RhoAV14 collected at the indicated periods were immunoblotted for M-cadherin, N-cadherin, β1-integrin, and α-tubulin expression. The data are representative of at least three independent experiments.

did not fuse (Figure 3B). Our R-cadherin RNAi was previously validated in a rhabdomyosarcoma-derived cell line (Charrasse *et al*., 2004), and it does not perturb the expression of the myogenic markers described above (our unpublished data). Quantification of the number of transfected cells that have fused in these two conditions is shown in Figure 3C.

Expression of Constitutively Active RhoA GTPase Specifically Modifies M-Cadherin Expression and Localization

Because we showed that active RhoA inhibits myoblast fusion (Figure 2) and that M-cadherin is required for this process (Figure 3), we next examined M-cadherin expression and localization in RhoA V14-expressing cells. Expression of M-cadherin was monitored at different times after the shift to DM. In control C2C12, M-cadherin is expressed throughout myogenesis and starts to decrease at day 3 (D3) (Figure 4). In RhoAV14-expressing cells, M-cadherin is decreased and has disappeared around D3. We often see a lower molecular weight band in RhoAV14-expressing cells that might result from dephosphorylation or proteolytic cleavage of M-cadherin (Zeschnigk *et al*., 1995). In contrast, RhoA V14 did not affect N-cadherin, β1-integrin, and tubulin expression levels as well as ADAM-12 (our unpublished data). We then analyzed M-cadherin localization by immunocytochemistry (Figure 5A). In control proliferating C2C12 myoblasts, M-cadherin accumulates at intercellular contacts (Figure 5A, a). After 2 d in differentiation medium, M-cadherin accumulates at myoblast-myotube and myotube-myotube contacts (Figure 5A, b). This agrees with data obtained in rat myoblasts (Eng *et al*., 1997). In RhoAV14-expressing cells, M-cadherin no longer accumulates at contacts between proliferating cells (Figure 5A, c) or cells in DM (Figure 5A, d). We used a biotinylation assay to further analyze the presence of M-cadherin at the cell surface. We analyzed total and cell surface biotinylated M-cadherin in control and RhoAV14-expressing C2C12 myoblasts cultured in growth or differentiation medium for the indicated period of time (Figure 5B). The histogram shows the level of biotinylated M-cadherin normalized to the amount of total cellular M-cadherin. From these data we conclude that, in RhoAV14-expressing myoblasts, the amount of M-cadherin at the plasma membrane is decreased. In contrast, the amount of N-cadherin at the plasma membrane is not modified by RhoAV14 expression (our unpublished data).

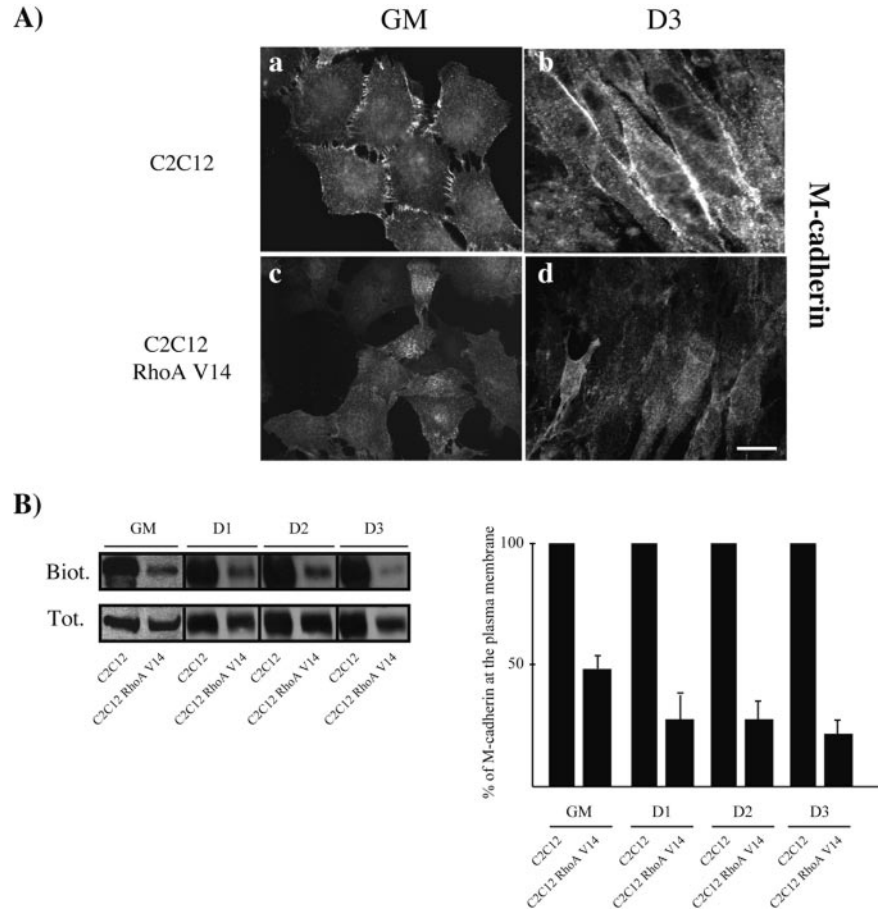

Figure 5. Effect of RhoAV14 on M-cadherin localization. (A) M-cadherin localization analyzed by indirect immunofluorescence in control C2C12 and C2C12 RhoAV14 proliferating myoblasts (a and c) or after 3 d in differentiation medium (b and d). Bar, 10 μm. (B) Confluent C2C12 and C2C12 RhoAV14 cultured in growth or differentiation medium were cell surface biotinylated at 4°C. Biotinylated cell surface M-cadherin was recovered on streptavidin beads. M-cadherin content in total (Tot) and biotinylated fractions (Biot) was analyzed by immunoblotting. The histogram represents the quantification of M-cadherin at the plasma membrane normalized for the total amount of M-cadherin calculated from at least three independent experiments.

RhoA Increases M-Cadherin Degradation through the Lysosomal Pathway

The results mentioned above demonstrate that RhoA induces the loss of M-cadherin and its delocalization from the cell surface. We then analyzed whether RhoA affects the turnover of M-cadherin. Control and RhoAV14-expressing myoblasts were treated with CHX, and the amount of M-cadherin was analyzed at different times. We also labeled control and RhoAV14-expressing myoblasts with [^{35}S]methionine/cysteine and performed pulse-chase experiments (Figure 6A). In both cases, we observed a strong decrease of M-cadherin stability in RhoA-expressing cells (Figure 6A). We also analyzed the subcellular localization of M-cadherin in control and RhoAV14-expressing myoblasts. Cells were stained with antibodies directed against the Golgi apparatus, endoplasmic reticulum, and endocytic, recycling, and degradation compartments. RhoA expression increases the colocalization of M-cadherin with the endocytic pathway (our unpublished data). To determine whether the internalized M-cadherin was degraded via a lysosomal pathway, we stained lysosomes by transfection of a plasmid encoding GFP-tagged CTNS (Figure 6B) or using LysoTracker dye (Figures 6C and 7B) (Kalatzis *et al*., 2001). In control cells, little colocalization between M-cadherin and CTNS was observed (Figure 6B, a–c). In contrast, RhoAV14 expression increased the colocalization of M-cadherin with CTNS (Figure 6B, d–f). Because the visualization of intracellular vesicular compartments is difficult in C2C12 myoblasts, HeLa cells were transfected with M-cadherin/GFP, incubated with LysoTracker dye, and analyzed by time-lapse confocal microscopy. As shown in Figure 6C and the accompanying videos, RhoAV14 increased the colocalization of M-cadherin/GFP with lysosomes. A quantitative analysis is shown in Figure 6D. To strengthen the observation of M-cadherin internalization through the endosome–lysosome pathway, C2C12 myoblasts were treated with chloroquine, an inhibitor of lysosomal activity, and analyzed for M-cadherin localization (Figure 7A). Chloroquine addition increased the vesicular accumulation of M-cadherin (Figure 7A, c), as in RhoAV14-expressing cells (compare Figure 7A, a and b). This treatment induced the appearance of large vesicular structures (as reported previously; Xiao *et al*., 2003) in which M-cadherin accumulates (Figure 7A, c). These vesicles correspond to lysosomes, as demonstrated by the analysis by time-lapse microscopy of M-cadherin/GFP-expressing C2C12 myoblasts incubated with LysoTracker dye to stain lysosomes. As shown in Figure 7B and the accompanying video, M-cadherin/GFP colocalized with lysosomes. To analyze whether lysosomes were involved in the decrease of M-cadherin levels in RhoAV14-expressing cells, the expression of M-cadherin in chloroquine-treated cells was analyzed by Western blot. In the presence of chloroquine we observe less down-regulation of M-cadherin in RhoAV14-expressing myoblasts (Figure 7A). No effect on M-cadherin expression levels or localization was detected after treatment with proteasomal inhibitors (our unpublished data).

Finally, we analyzed whether RhoA induces the ubiquitination of M-cadherin. Indeed, polyubiquitination targets proteins for the destruction by the proteasome, whereas monoubiquitination triggers internalization and degrada-

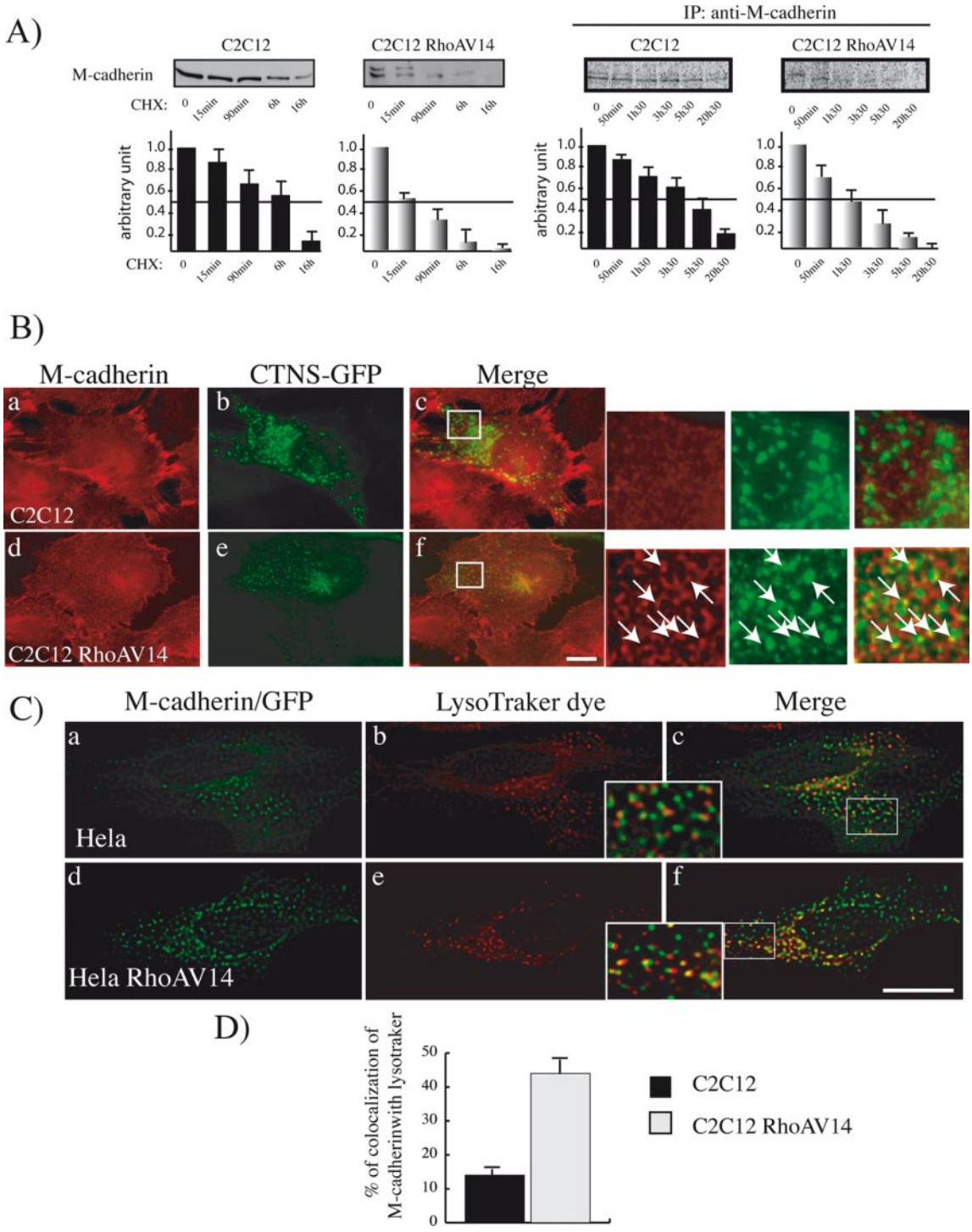

Figure 6. RhoA induces the degradation of M-cadherin. (A) C2C12 and C2C12 RhoAV14 myoblasts were treated with cycloheximide (10 μg/ml) for different times, and the level of M-cadherin protein was analyzed by Western blot. The histogram represents the quantification of M-cadherin protein level after cycloheximide treatment from three independent experiments. M-cadherin turnover was also examined by pulse-chase analysis of C2C12 and C2C12 RhoAV14 myoblasts. The histogram represents the quantification of M-cadherin protein level from four independent experiments. (B) Control and RhoAV14-expressing C2C12 myoblasts were transfected with CTNS-GFP (b and e) and stained for M-cadherin (a and d). c and f are the superimposition of the deconvolved images of a single plane of the M-cadherin and CTNS-GFP staining. Insets corresponding to the selected area in each panel are shown. Bar, 10 μm. (C) Control (a–c) and RhoAV14-expressing HeLa cells (d–f) were transfected with M-cadherin/GFP. Sixteen hours later, cells were incubated with LysoTracker dye, and the distribution of GFP (a and d) and rhodamine-labeled probes (b and e) was examined by time-lapse confocal microscopy. Images were captured every 2 s for 2 min, and stacks of images were deconvolved using the Huygens System image restoration software. c and f are the superimposition of the a/b and d/e panels, respectively. Insets corresponding to the selected area in each panel are shown. (D) Values represent the percentage of M-cadherin-containing vesicles colocalized with LysoTracker-labeled lysosomes calculated with the colocalization module of MetaMorph (version 6.2r5; Molecular Devices). The results are representative of two independent experiments.

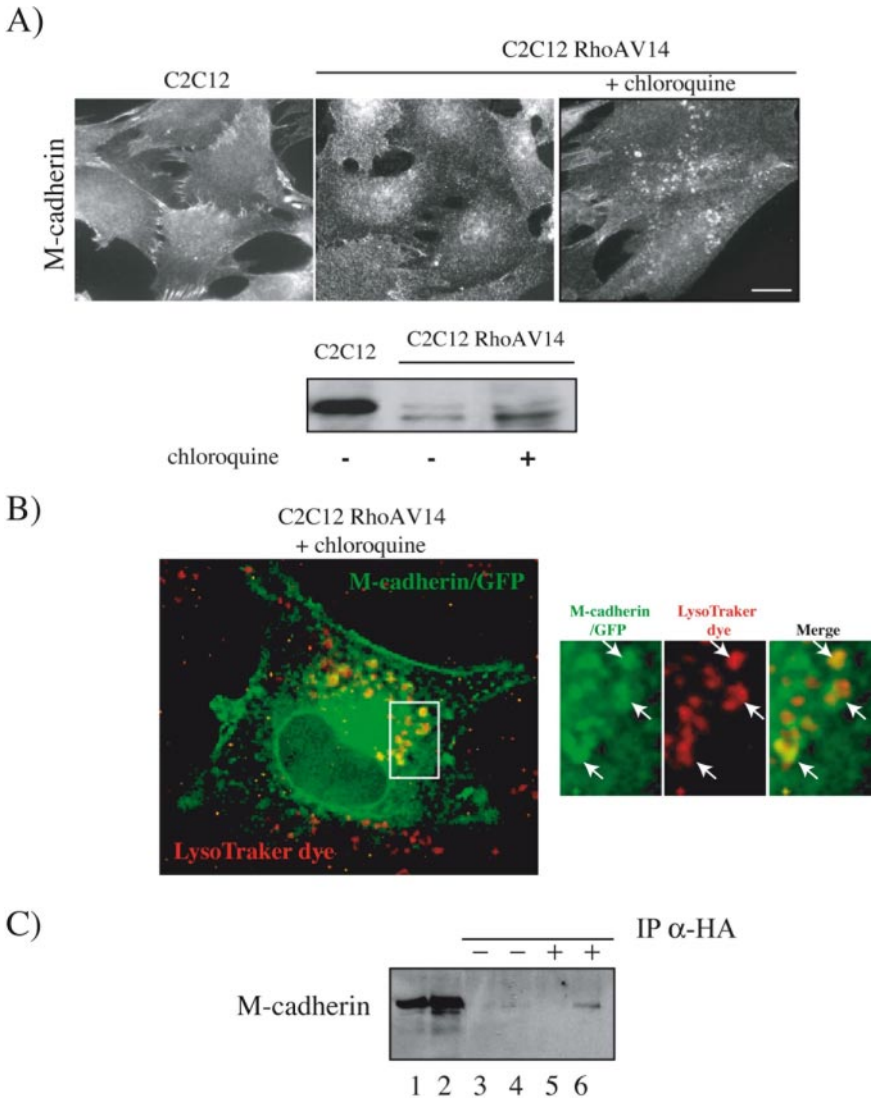

Figure 7. Treatment of cells with lysosomal inhibitors. (A) Control (a) and RhoAV14-expressing C2C12 myoblasts were either untreated (b) or treated with chloroquine for 6 h (c). M-cadherin was analyzed by immunocytochemistry and Western blot. (B) RhoAV14-expressing C2C12 myoblasts transfected with a vector for M-cadherin/GFP were treated with chloroquine for 6 h and incubated with LysoTracker dye. M-cadherin and lysosome distribution was examined by time-lapse microscopy. Images were captured every 10 s for 10 min, and stacks of images were deconvolved using the Huygens System image restoration software. One deconvolved plan is shown. Insets corresponding to the selected area are shown. (C) Control (lanes 1, 3, and 5) and RhoAV14-expressing C2C12 myoblasts (lanes 2, 4, and 6) were either untransfected (lanes 1 and 2) or cotransfected with HA-tagged ubiquitin, and a β-gal reporter gene to normalize transfection efficiency (lanes 3–6). M-cadherin was analyzed by Western blot after immunoprecipitation of HA-tagged proteins. −, without anti-HA antibody (lanes 3 and 4); +, with anti-HA antibody (lanes 5 and 6).

tion in lysosomes (Hicke, 2001). The level of ubiquitinated M-cadherin was analyzed by immunoprecipitation of ubiquinated proteins from control (Figure 7C, lanes 3 and 5) and RhoAV14-expressing myoblasts (lanes 4 and 6) transfected with HA-tagged ubiquitin. Expression of RhoAV14 increased the amount of monoubiquitination of M-cadherin. We were unable to detect any N-cadherin ubiquitination either in control or in RhoAV14-expressing myoblasts, showing this is event is specific for M-cadherin (our unpublished data).

RhoA Affects the Association of M-Cadherin with p120 Catenin

To characterize the mechanism by which RhoA is acting, we analyzed the expression level of p120 catenin and its association with M-cadherin. Recent reports suggest that p120 plays a gatekeeper function in determining the fate of cadherin by regulating its delivery to and its stability at the cell surface (Peifer and Yap, 2003). We first observed that p120 levels are maintained throughout myogenesis and are not affected by RhoA expression (Figure 8A). In contrast, the expression of RhoAV14 strongly decreases the association of p120 catenin with M-cadherin (Figure 8B). p120 catenin association with M-cadherin is higher around myoblast fusion, suggesting the formation or the reinforcement of a complex containing these proteins at this time. p120 catenin association with N-cadherin is observed throughout myogenesis and RhoAV14 expression has only a little effect on the association of p120 catenin with N-cadherin (Figure 8B). To visualize this, control and RhoAV14-expressing myoblasts were stained with antibodies directed against p120 catenin and either M-cadherin or N-cadherin. As shown in Figure 8C, the expression of RhoAV14 perturbed M-cadherin accumulation at intercellular contacts (compare Figure 8C, a and c). By contrast, N-cadherin and p120 catenin still accumulated at intercellular contacts (compare Figure 8C, b and d, e and g, and f and h). To elucidate the molecular mechanisms by which RhoA might regulate p120 catenin association with M-cadherin, we studied a RhoA effector, the serine/threonine kinase ROCK/ROK. We tested the effect of Y-27632, a pharmacological ROCK inhibitor, on p120 catenin association with M-cadherin. As shown in Figure 9A, Y-27635 restores partially p120 catenin association with M-cadherin in RhoAV14-expressing cells. Moreover, Y-27632 addition to RhoAV14-expressing cells restored the localization of M-cadherin at the cell–cell contact sites (Figure 9B).

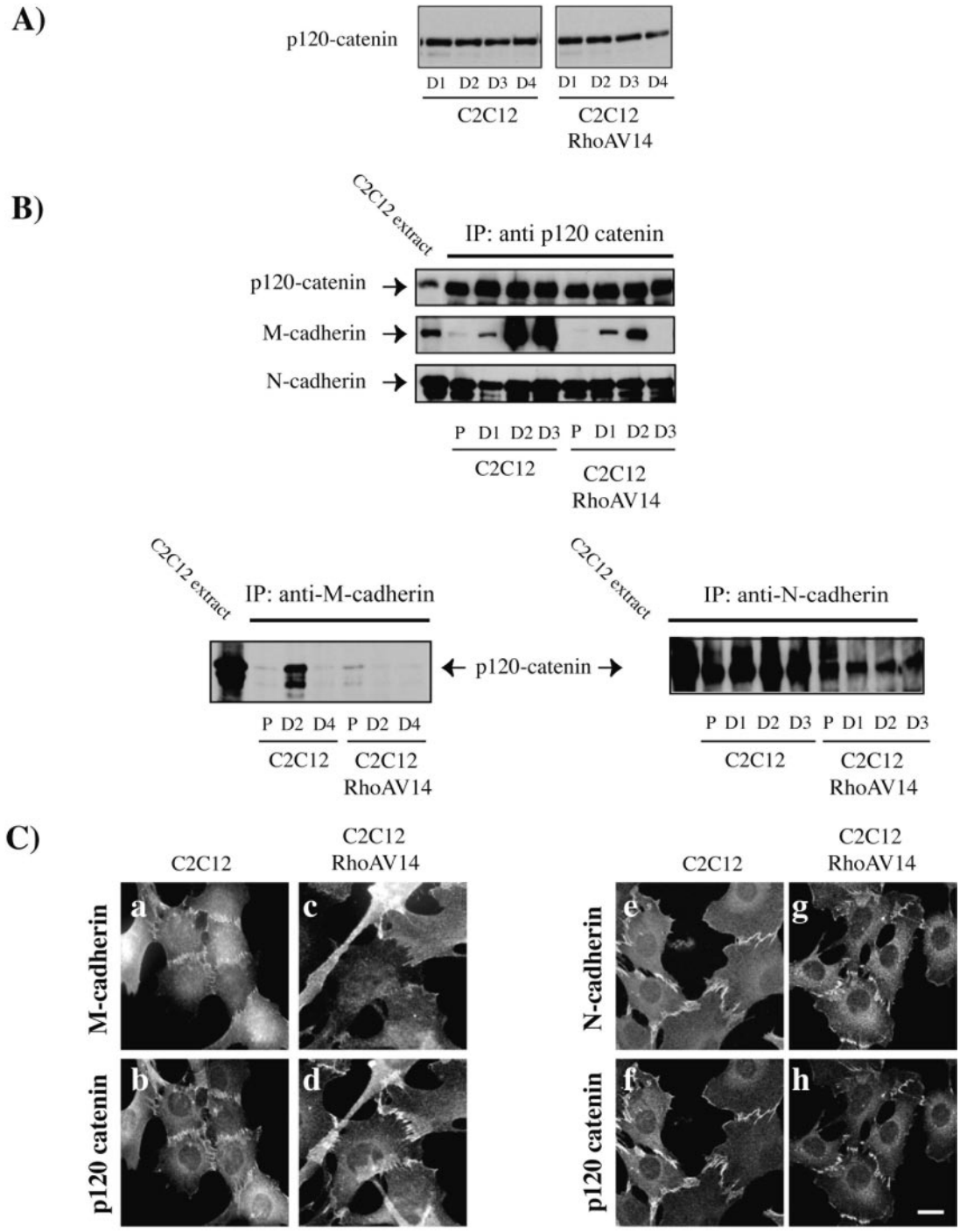

Figure 8. RhoA impairs p120 association to M-cadherin. (A) Cell lysate (20 μg) of control and RhoAV14-expressing C2C12 myoblasts collected at different times after differentiation medium addition (from D1 to D4) were analyzed by Western blot for p120 catenin expression. (B) Cell lysates of control and RhoAV14-expressing C2C12 myoblasts collected at different times after differentiation medium addition (from D1 to D4) were immunoprecipitated using an anti-p120 catenin antibody and immunoblotted for the presence of p120 catenin, M-cadherin, and N-cadherin (top). Cell lysates of control and RhoAV14-expressing C2C12 myoblasts collected at different times after addition of differentiation medium were immunoprecipitated using either an anti-M-cadherin (bottom left) or anti-N-cadherin antibody (bottom right) and immunoblotted for the presence of p120 catenin. (C) Control C2C12 (a, b, e, and f) and C2C12 RhoAV14-expressing myoblasts (c, d, g, and h) were stained with antibodies against p120 catenin (b, d, f, and h) and either M-cadherin (a and e) or N-cadherin (e and g). Bar, 10 μm.

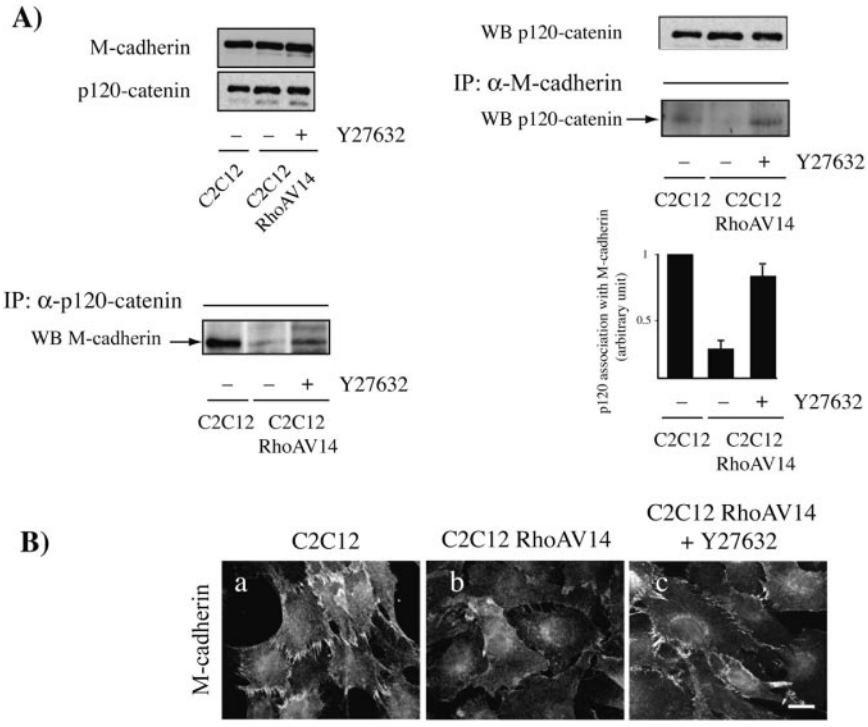

Figure 9. Effect of ROCK inhibitor. (A) Cell lysates of control and RhoAV14-expressing C2C12 myoblasts treated or not with the ROCK inhibitor Y-27632 were analyzed by Western blot for M-cadherin and p120 catenin expression (left top) or immunoprecipitated using an anti-M-cadherin antibody and immunoblotted for the presence of p120 catenin (right). The histogram shows the quantification of p120 association with M-cadherin from three independent experiments. The same lysates were also immunoprecipitated using an anti-p120 catenin antibody and immunoblotted for the presence of M-cadherin (left bottom). (B) M-cadherin localization was analyzed by indirect immunofluorescence in control C2C12 (a) and C2C12 RhoAV14-expressing myoblasts treated (c) or not (b) with the ROCK inhibitor Y-27632. Bar, 10 μm.

DISCUSSION

Skeletal myogenesis is a multistep process that is regulated both temporally and spatially and that requires cell–cell interaction at various steps. In this study, we have shown that M-cadherin is required for myoblast fusion into myotubes. This corroborates a previous study that inhibited M-cadherin activity using antagonistic peptides and expression of antisense RNA (Zeschnigk *et al*., 1995). Nevertheless, this study used L6 myoblasts that lack N-cadherin, which raises the possibility that, when coexpressed in cells, both molecules might contribute to the control of myoblast fusion. Here, we used mouse C2C12 myoblasts, which express M- and N-cadherin, and showed that M-cadherin inhibition by RNA interference specifically abrogated myoblast fusion. Thus, N-cadherin cannot compensate for M-cadherin in myoblastic cell lines, unlike the situation in vivo (Hollnagel *et al*., 2002). We have previously shown that N-cadherin function is required for induction of myogenesis (Charrasse *et al*., 2002); here, we find that M-cadherin controls myoblast fusion without affecting induction of myogenesis. This validates C2C12 myoblasts as a model to study the respective role of N- and M-cadherin in these two important steps of myogenesis. Why the compensatory mechanism observed in vivo does not function in these cell lines remains unclear. Another important question concerns the exact function of M-cadherin during fusion of myoblasts into myotubes. Myoblast fusion results from an ordered sequence of events, including cell migration, alignment, recognition, adhesion, and membrane merging. Anything that hinders one of these steps would likely decrease the fusion rate.

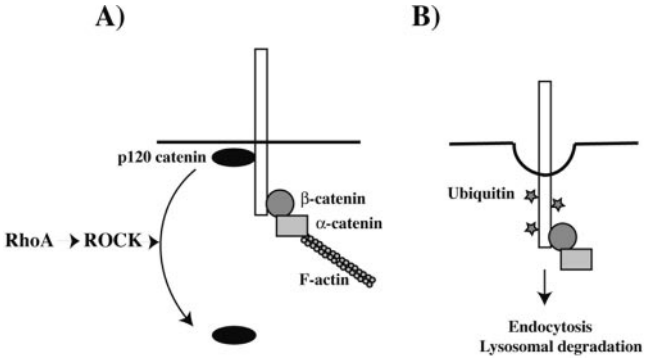

Figure 10. Model of the suggested RhoA effect on M-cadherin. Sustained activation of RhoA induces the dissociation of p120 catenin from M-cadherin (A); thus, M-cadherin is monoubiquitinated and then endocytosed and degraded through a lysosomal pathway (B).

Our results establish that RhoA activity must be down-regulated to allow fusion to occur. Indeed, we have observed that maintaining a high RhoA activity impairs myoblast fusion in a variety of myoblast cell lines (Meriane *et al*., 2000), and this was recently confirmed in C2C12 myoblasts by others (Nishiyama *et al*., 2004). This idea is also supported by the decrease of Rho activity we observed at the onset of myoblast fusion. Thus, RhoA GTPase activity seems to be tightly controlled throughout myogenesis to allow its completion. At the very beginning of myogenesis, RhoA is activated through an N-cadherin-mediated pathway (Charrasse *et al*., 2002), before being down-regulated at the onset of myoblast fusion. The mechanisms responsible for the decrease of RhoA activity at the onset of myoblast fusion remain to be determined. This decrease of RhoA activity is required for the correct function of M-cadherin. Because its inhibition blocks the fusion process, the decrease in M-cadherin might fully explain the lack of fusion we observed in RhoAV14-expressing cells. Attempts to rescue the fusion process by coexpressing exogenous M-cadherin with RhoAV14 have not been successful, because both endogenous and overexpressed M-cadherin were degraded (our unpublished data). Nevertheless, other molecules participat-

ing in muscle cell fusion might be affected. This is not the case for β1-integrin and ADAM-12; however, the nuclear accumulation of the transcription factor Forked in human rhabdomyosarcoma is impaired in RhoAV14-expressing cells (Nishiyama *et al*., 2004).

Furthermore, our data show that sustained RhoA activity leads to the ubiquitination of M-cadherin, resulting in its entry into endocytic vesicles and its degradation by the lysosomal pathway. A similar process has been described for E-cadherin in response to the activation of the tyrosine kinase src (Fujita *et al*., 2002; Palacios *et al*., 2005). This was proposed to be an important posttranscriptional mechanism that could be operational during tumor progression and metastases as well as during some processes of normal development. M-cadherin ubiquitination and endocytosis in RhoAV14-expressing cells might result from its failure to associate with p120 catenin (Figure 10). Indeed, endocytosis has emerged as a regulatory mechanism that modulates cadherin cell surface levels in cells (Le *et al*., 1999; Akhtar and Hotchin, 2001; Palacios *et al*., 2002), and recent reports have shown that p120 catenin controls VE-cadherin internalization and degradation (Xiao *et al*., 2003). Thus, p120 is a regulator of cell–cell adhesion through the maintenance of cadherin levels in cells (Ireton *et al*., 2002; Davis *et al*., 2003; Peifer and Yap, 2003). Nevertheless, RhoAV14 expression specifically dissociates p120 from M-cadherin without similar effect on N-cadherin. This suggests the existence of specific interplay between the modified form of p120 or different p120 isoforms with N- and M-cadherin. The function of p120 catenin in regulating adhesion is probably controlled by phosphorylation both on tyrosine and serine/threonine residues (Mariner *et al*., 2001; Xia *et al*., 2003). Interestingly, we have found that the inhibition of the RhoA effector ROCK partially restores p120 catenin association with M-cadherin and the localization of M-cadherin at cell–cell contact sites. In our hands, ROCK inhibition does not relieve the block of myoblast fusion in C2C12 myoblasts expressing RhoAV14, in contrast to recent data (Nishiyama *et al*., 2004). Further experiments are necessary to both determine which other pathway(s) downstream of RhoA participate in the process of myoblast fusion and also to identify the targets of ROCK; however, it is fair to speculate that p120 catenin and/or M-cadherin are good candidates.

The identification of a pathway by which RhoA inhibits M-cadherin function will prove useful in understanding the molecular mechanisms involved in muscle diseases where fusion is affected or during the repair process that involves adult satellite–cell fusion.

ACKNOWLEDGMENTS

We thank Pierre Travo and Sylvain De Rossi for constant support (http://www.mri.cnrs.fr/), Bob Hipskind for critical reading of the manuscript, and Olivier Coux for discussions. We also thank Guillaume Fargier for technical support. This work was supported by the Ligue Nationale Contre le Cancer (équipe labelisée), the Association Francaise pour la Recherche contre le Cancer, and the Association Francaise contre les Myopathies.

REFERENCES

Akhtar, N., and Hotchin, N. A. (2001). RAC1 regulates adherens junctions through endocytosis of E-cadherin. Mol. Biol. Cell *12*, 847–862.

Andres, V., and Walsh, K. (1996). Myogenin expression, cell cycle withdrawal, and phenotypic differentiation are temporally separable events that precede cell fusion upon myogenesis. J. Cell Biol. *132*, 657–666.

Bahjaoui-Bouhaddi, M., Padilla, F., Nicolet, M., Cifuentes-Diaz, C., Fellmann, D., and Mege, R. M. (1997). Localized deposition of M-cadherin in the glomeruli of the granular layer during the postnatal development of mouse cerebellum. J. Comp. Neurol. *378*, 180–195.

Bornemann, A., and Schmalbruch, H. (1994). Immunocytochemistry of M-cadherin in mature and regenerating rat muscle. Anat. Rec. *239*, 119–125.

Carnac, G., Primig, M., Kitzmann, M., Chafey, P., Tuil, D., Lamb, N., and Fernandez, A. (1998). RhoA GTPase and serum response factor control selectively the expression of MyoD without affecting Myf5 in mouse myoblasts. Mol. Biol. Cell *9*, 1891–1902.

Charlton, C. A., Mohler, W. A., and Blau, H. M. (2000). Neural cell adhesion molecule (NCAM) and myoblast fusion. Dev. Biol. *221*, 112–119.

Charrasse, S., Causeret, M., Comunale, F., Bonet-Kerrache, A., and Gauthier-Rouviere, C. (2003). Rho GTPases and cadherin-based cell adhesion in skeletal muscle development. J. Muscle Res. Cell Motil. *24*, 309–313.

Charrasse, S., Comunale, F., Gilbert, E., Delattre, O., and Gauthier-Rouviere, C. (2004). Variation in cadherins and catenins expression is linked to both proliferation and transformation of Rhabdomyosarcoma. Oncogene *23*, 2420–2430.

Charrasse, S., Meriane, M., Comunale, F., Blangy, A., and Gauthier-Rouviere, C. (2002). N-Cadherin-dependent cell-cell contact regulates Rho GTPases and beta-catenin localization in mouse C2C12 myoblasts. J. Cell Biol. *158*, 953–965.

Chen, E. H., and Olson, E. N. (2004). Towards a molecular pathway for myoblast fusion in *Drosophila*. Trends Cell Biol. *14*, 452–460.

Cifuentes-Diaz, C., Goudou, D., Padilla, F., Facchinetti, P., Nicolet, M., Mege, R. M., and Rieger, F. (1996). M-cadherin distribution in the mouse adult neuromuscular system suggests a role in muscle innervation. Eur. J. Neurosci. *8*, 1666–1676.

Cifuentes-Diaz, C., Nicolet, M., Alameddine, H., Goudou, D., Dehaupas, M., Rieger, F., and Mege, R. M. (1995). M-cadherin localization in developing adult and regenerating mouse skeletal muscle: possible involvement in secondary myogenesis. Mech. Dev. *50*, 85–97.

Davis, M. A., Ireton, R. C., and Reynolds, A. B. (2003). A core function for p120-catenin in cadherin turnover. J. Cell Biol. *163*, 525–534.

Doberstein, S. K., Fetter, R. D., Mehta, A. Y., and Goodman, C. S. (1997). Genetic analysis of myoblast fusion: blown fuse is required for progression beyond the prefusion complex. J. Cell Biol. *136*, 1249–1261.

Donalies, M., Cramer, M., Ringwald, M., and Starzinski-Powitz, A. (1991). Expression of M-cadherin, a member of the cadherin multigene family, correlates with differentiation of skeletal muscle cells. Proc. Natl. Acad. Sci. USA *88*, 8024–8028.

Dworak, H. A., and Sink, H. (2002). Myoblast fusion in *Drosophila*. Bioessays *24*, 591–601.

Eng, H., Herrenknecht, K., Semb, H., Starzinski-Powitz, A., Ringertz, N., and Gullberg, D. (1997). Effects of divalent cations on M-cadherin expression and distribution during primary rat myogenesis in vitro. Differentiation *61*, 169–176.

Fazeli, S., Wells, D. J., Hobbs, C., and Walsh, F. S. (1996). Altered secondary myogenesis in transgenic animals expressing the neural cell adhesion molecule under the control of a skeletal muscle alpha-actin promoter. J. Cell Biol. *135*, 241–251.

Fujita, Y., Krause, G., Scheffner, M., Zechner, D., Leddy, H. E., Behrens, J., Sommer, T., and Birchmeier, W. (2002). Hakai, a c-Cbl-like protein, ubiquitinates and induces endocytosis of the E-cadherin complex. Nat. Cell Biol. *4*, 222–231.

Gauthier-Rouviere, C., Vignal, E., Meriane, M., Roux, P., Montcourier, P., and Fort, P. (1998). RhoG GTPase controls a pathway that independently activates Rac1 and Cdc42Hs. Mol. Biol. Cell *9*, 1379–1394.

Hicke, L. (2001). Protein regulation by monoubiquitin. Nat. Rev. Mol. Cell. Biol. *2*, 195–201.

Hollnagel, A., Grund, C., Franke, W. W., and Arnold, H. H. (2002). The cell adhesion molecule M-cadherin is not essential for muscle development and regeneration. Mol. Cell. Biol. *22*, 4760–4770.

Huovila, A. P., Almeida, E. A., and White, J. M. (1996). ADAMs and cell fusion. Curr. Opin. Cell Biol. *8*, 692–699.

Ireton, R. C., *et al*. (2002). A. novel role for p120 catenin in E-cadherin function. J. Cell Biol. *159*, 465–476.

Kalatzis, V., Cherqui, S., Antignac, C., and Gasnier, B. (2001). Cystinosin, the protein defective in cystinosis, is a H(+)-driven lysosomal cystine transporter. EMBO J. *20*, 5940–5949.

Kuch, C., Winnekendonk, D., Butz, S., Unvericht, U., Kemler, R., and Starzinski-Powitz, A. (1997). M-cadherin-mediated cell adhesion and complex formation with the catenins in myogenic mouse cells. Exp. Cell Res. *232*, 331–338.

Le, T. L., Yap, A. S., and Stow, J. L. (1999). Recycling of E-cadherin: a potential mechanism for regulating cadherin dynamics. J. Cell Biol. *146*, 219–232.

Mariner, D. J., Anastasiadis, P., Keilhack, H., Bohmer, F. D., Wang, J., and Reynolds, A. B. (2001). Identification of Src phosphorylation sites in the catenin p120ctn. J. Biol. Chem. *276*, 28006–28013.

Mary, S., Charrasse, S., Meriane, M., Comunale, F., Travo, P., Blangy, A., and Gauthier-Rouviere, C. (2002). Biogenesis of N-cadherin-dependent cell-cell contacts in living fibroblasts is a microtubule-dependent kinesin-driven mechanism. Mol. Biol. Cell *13*, 285–301.

Meriane, M., Roux, P., Primig, M., Fort, P., and Gauthier-Rouviere, C. (2000). Critical activities of Rac1 and Cdc42Hs in skeletal myogenesis: antagonistic effects of JNK and p38 pathways. Mol. Biol. Cell *11*, 2513–2528.

Moore, R., and Walsh, F. S. (1993). The cell adhesion molecule M-cadherin is specifically expressed in developing and regenerating, but not denervated skeletal muscle. Development *117*, 1409–1420.

Nishiyama, T., Kii, I., and Kudo, A. (2004). Inactivation of Rho/ROCK signalling is crucial for the nuclear accumulation of FKHR and myoblast fusion. J. Biol. Chem. *279*, 47311–47319.

Palacios, F., Schweitzer, J. K., Boshans, R. L., and D'Souza-Schorey, C. (2002). ARF6-GTP recruits Nm23–H1 to facilitate dynamin-mediated endocytosis during adherens junctions disassembly. Nat. Cell Biol. *4*, 929–936.

Palacios, F., Tushir, J. S., Fujita, Y., and D'Souza-Schorey, C. (2005). Lysosomal targeting of E-cadherin: a unique mechanism for the down-regulation of cell-cell adhesion during epithelial to mesenchymal transitions. Mol. Cell. Biol. *25*, 389–402.

Peifer, M., and Yap, A. S. (2003). Traffic control: p120-catenin acts as a gatekeeper to control the fate of classical cadherins in mammalian cells. J. Cell Biol. *163*, 437–440.

Pouliot, Y., Gravel, M., and Holland, P. C. (1994). Developmental regulation of M-cadherin in the terminal differentiation of skeletal myoblasts. Dev. Dyn. *200*, 305–312.

Rose, O., Rohwedel, J., Reinhardt, S., Bachmann, M., Cramer, M., Rotter, M., Wobus, A., and Starzinski-Powitz, A. (1994). Expression of M-cadherin protein in myogenic cells during prenatal mouse development and differentiation of embryonic stem cells in culture. Dev. Dyn. *201*, 245–259.

Rosen, G. D., Sanes, J. R., LaChance, R., Cunningham, J. M., Roman, J., and Dean, D. C. (1992). Roles for the integrin VLA-4 and its counter receptor VCAM-1 in myogenesis. Cell *69*, 1107–1119.

Schwander, M., Leu, M., Stumm, M., Dorchies, O. M., Ruegg, U. T., Schittny, J., and Muller, U. (2003). Beta1 integrins regulate myoblast fusion and sarcomere assembly. Dev. Cell *4*, 673–685.

Taylor, M. V. (2000). Muscle development: molecules of myoblast fusion. Curr. Biol. *10*, R646–R648.

Taylor, M. V. (2002). Muscle differentiation: how two cells become one. Curr. Biol. *12*, R224–R228.

Wei, L., Zhou, W., Croissant, J. D., Johansen, F. E., Prywes, R., Balasubramanyam, A., and Schwartz, R. J. (1998). RhoA signaling via serum response factor plays an obligatory role in myogenic differentiation. J. Biol. Chem. *273*, 30287–30294.

Xia, X., Mariner, D. J., and Reynolds, A. B. (2003). Adhesion-associated and protein kinase C-modulated changes in serine/threonine phosphorylation of p120-catenin. Biochemistry *42*, 9195–9204.

Xiao, K., Allison, D. F., Buckley, K. M., Kottke, M. D., Vincent, P. A., Faundez, V., and Kowalczyk, A. P. (2003). Cellular levels of p120 catenin function as a set point for cadherin expression levels in microvascular endothelial cells. J. Cell Biol. *163*, 535–545.

Zeschnigk, M., Kozian, D., Kuch, C., Schmoll, M., and Starzinski-Powitz, A. (1995). Involvement of M-cadherin in terminal differentiation of skeletal muscle cells. J. Cell Sci. *108*, 2973–2981.